

## BASE ISOLATION FOR SEISMIC PROTECTION OF STATUES

Fabrizio VESTRONI<sup>1</sup> And Simone DI CINTIO<sup>2</sup>

### SUMMARY

This paper deals with base isolation as the technique to minimize the seismic risk for statues. The isolating device is created by providing multi-stage high damping laminated rubber bearings. The response of the isolated system has been studied in frequency-domain and time-domain, using generated and recorded accelerograms. First, reference is made to a linearized model of the devices. In view of these latest results, the response of isolated system has been studied as a SDOF system characterized by an hysteretic force-displacement law; a parametric analysis has been performed to determine the sensitivity of the response to the characteristics of devices and seismic forces. Benefits of base isolation have been shown with reference to displacement and maximum base shear.

### INTRODUCTION

Scientific community agrees about the fact that base isolation by means of high damping laminated rubber bearings provides interesting solutions for a wide series of applications. Reliability of such a system is nowadays proofed by a large number of applications, even very old ones, regarding many large structures like public buildings, nuclear plants, bridges, etc. [1].

In this paper base isolation as the technique to minimize the seismic risk for important statues and similar works is studied. Statues of archaeological site of Villa Adriana in Tivoli (Italy) have been taken as reference. National and international regulations and guidelines for isolated structures [2] cannot be ignored for the design of the isolation system. It should be noted that the statue to be isolated is a completely different system compared to the conventional structures, because of material, mass, shape and overall dimensions. In this case base isolation is important because the system is very stiff and therefore likely exposed to high seismic forces. Since the small mass of the statue, highly deformable isolators having small cross-section area have to be used: it is thus important to test them carefully in order to determine exactly their stability under design seismic forces. The particular kind of structure, a statue, does not allow any reduction of design forces, based on post-elastic behavior of the structure, and a specific seismic input for the design of the isolation system is to be determined.

The aim of the analysis is the design of the isolation devices: the analysis has been conducted in a parametric way, by varying number of isolators and shear module of rubber utilized.

The response of a spatial model of the system, where isolators are represented by equivalent linear viscous elements, is studied. It is shown that a good description of such a system can be obtained by using a SDOF system, having an hysteretic force-displacement law characterized by parameters determined by comparing model and experimental results. Using this model the response of the base isolated system is determined, and the efficiency of the seismic protection technique used is verified.

<sup>1</sup> Department of Structural and Geotechnical Engineering, "La Sapienza" University, Rome, Italy

<sup>2</sup> Architects, Planners, Consulting Engineers "The OK Design Group", Rome, Italy

## DEFINITION OF SEISMIC INPUT

Nowadays seismic properties of the site where the system to be isolated stands should always been studied carefully. Current Italian regulations define directly a design spectra with an assigned value of damping coefficient  $\alpha$ , instead of suggesting a general-purpose elastic spectra. The first one can be used only for linear analysis of structures having good nonlinear dissipation properties as, for example, space-frame structure buildings having good overall ductility. An hazard evaluation has been performed and the results have been compared with available historic seismic information, international seismic regulations and most recent guidelines and codes for seismic isolated structures.

The method used to determine site seismic hazard, originally proposed by Cornell (1968), is based on the following assumptions: *a*) frequency of earthquakes follows Poisson statistical distribution: the events are stationary and independent one each other; *b*) a recurrence law applies between number of events and their intensity; *c*) seismic activity inside an area is uniform, earthquakes have same probability to occur within the area and they follow the same frequency law. This method involves use of a seismic zonation (Scandone, 1996), a seismic catalog (Camassi and Stucchi, 1996), the Gutenberg-Richter recurrence law, and an attenuation law (Sabetta and Pugliese) [3].

Results of the analysis are shown in Fig. 1*a*, where uniform hazard spectra is compared to the Eurocode [4] spectra for stiff soils (EC8-A) scaled in order to fit the first one in the two important ranges of frequencies of the system: constant velocity portion ( $T > 0.4$  sec), for the design of the isolation system, and high frequencies portion ( $T < 0.1$  sec), to check actual conditions of statues. Best matching of the hazard spectra is obtained with effective peak ground acceleration of EC8-A,  $a_g = 0.18$  g.

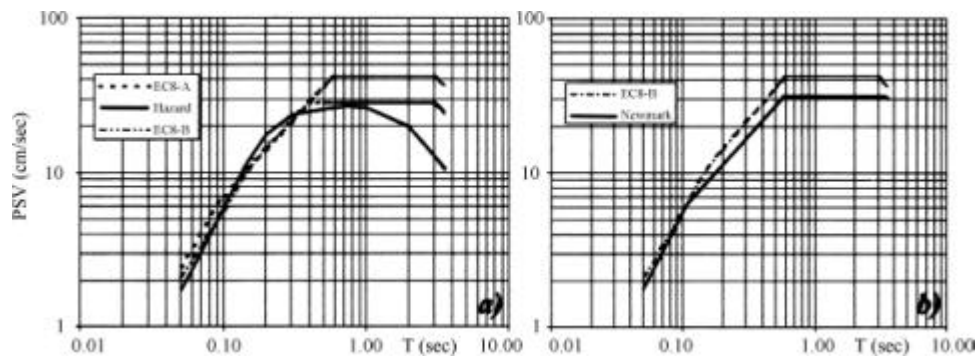


**Figure 1. Comparison between uniform hazard spectrum, Eurocode spectra for stiff soils, EC8-A, and medium soils, EC8-B (a). Comparison between specific site elastic spectrum and reference spectrum, EC8-B (b).**

To take into account seismic forces modification due to the upper (soft to medium) layers of soil, EC8-B spectrum, given for medium soils, has been taken as the reference earthquake. It is shown in Fig. 1*a* together with the above ones, both regarding stiff soil conditions: the assumption of medium soil conditions makes pseudo-velocity (*PSV*) values higher at the low frequencies, lower at the very high frequencies. Since the isolated structure is characterized by an high period, EC8-B spectrum is certainly conservative. According to the available historic information, the maximum seismic intensity occurred in the area of Tivoli is VIII (*MCS* System). By using correlations available in literature to estimate motion peak values, and following the procedure proposed by Newmark [5], a deterministic elastic spectrum has been determined. This spectrum, representative of real condition of the site, is compared, in Fig. 1*b*, to the reference spectrum. It can be noted that the latter is more conservative: deterministic analysis, conducted taking into account the specific site characteristics, therefore supports the choice of the reference earthquake made before.

To represent seismic forces in time-domain, a set of twelve artificial accelerograms compatible with the assigned spectrum (see, for example, Fig. 2) has been generated by using Simqke code, and a set of eight recorded accelerograms (Fig. 3), suitable to the investigation of the system considered, have been selected from an ensemble of sixty recent Italian accelerograms, occurred in the period 1976-1984.

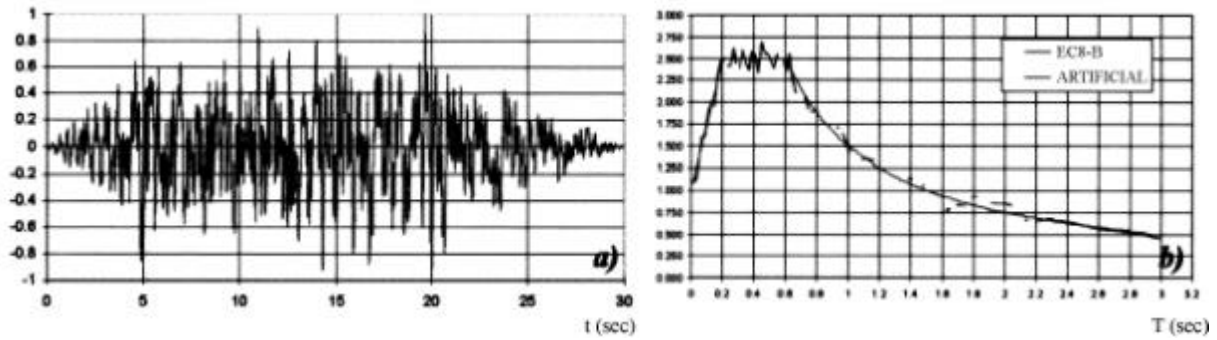


Figure 2. Example of generated compatible accelerogram (a) and associated response spectrum (b).

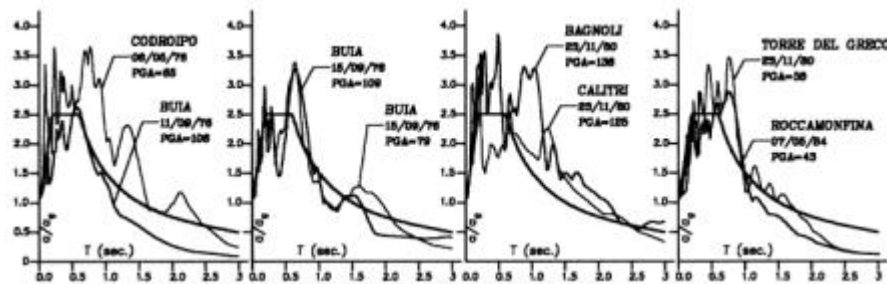


Figure 3. Response spectra of recorded accelerograms.

### DYNAMICAL CHARACTERIZATION OF THE SYSTEM AND LINEAR RESPONSE

The reference statue is 2.14 m high, including the base (11 cm) and the capital (22 cm); the base is 63x53 centimeters. The total weight of the work is 1050 Kg. Masses are mainly symmetric with reference to a central vertical axis: forearms, disk, and garment produce some minor exceptions. Realistic values for properties of marble used are:  $\rho_m=2700 \text{ kg/m}^3$ ,  $E_m=7 \times 10^3 \text{ kg/m}^2$ ,  $G_m=2.8 \times 10^3 \text{ kg/m}^2$ ,  $\nu_m=0.25$ . The isolating device is created by providing high damping laminated rubber bearings according to previous experiences [6]: these isolators are on different layers, connected by steel plates, as already proposed in [7]. Main features of these devices are: high axial compression stiffness, horizontal stiffness decreasing with increasing deformations, good dissipation properties, long estimated average lifetime. A front view of the statue and the geometry of isolation system are shown in Fig. 4. Static and dynamic tests on elastomeric isolators [8] show a limited influence of vibration frequency on dissipated energy. This means that damping properties of the isolators are due to an hysteretic behavior rather than a viscous one. For this reason, both a linear analysis with equivalent viscous damping and a nonlinear analysis using an hysteretic model have been carried out.

In order to determine dynamical properties of the isolated system (*IS*) and to perform a conventional seismic analysis, a linear space model of statue and isolation system has been generated. For each isolator a linear equivalent force-displacement relationship has been adopted, with stiffness equal to the secant stiffness at 100% of strain (Fig. 5), and viscous damping such that energy dissipation in a cycle with a strain amplitude of 100% and a frequency near to the system first frequency is the same. Dynamical characterization of the system has confirmed the good potentialities of the base-isolation. In *IS*, first mode shapes involve only deformations of isolators, while the statue shows only rigid motion; participating mass in *Y* and *X* translations (first two modes) are more than 97% in *IS*, against values of about 68% in non-isolated system (*NIS*); periods of first two modes of *IS* are in the range 1.5-1.6 sec against 0.08 sec for *NIS* (Fig. 6, left).

First of all, response of *NIS* has been determined, based on an assigned spectrum. This analysis has shown the unsuitability of the statue actual conditions in resisting strong earthquakes. The isolation system has been chosen on the basis of the response of *IS*, using the reference spectrum analysis, by varying number of isolators and shear module of rubber. The response of the best system (three isolating layers, soft rubber) has been analyzed in time-domain and frequency-domain, by using the 12 generated accelerograms, the 8 recorded ones, and their associated response spectra. With the two sets of accelerograms it has been so possible to compare the two kinds of analysis, and to understand the behavior of the system under motions with different frequency contents.

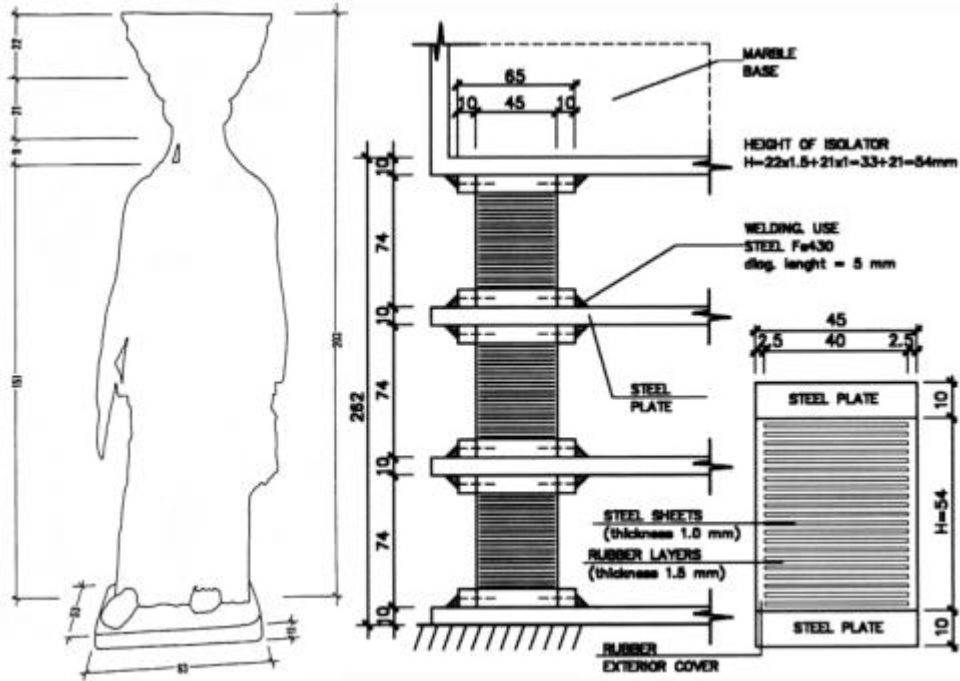


Figure 4. Front view of the statue and geometry of isolation system.

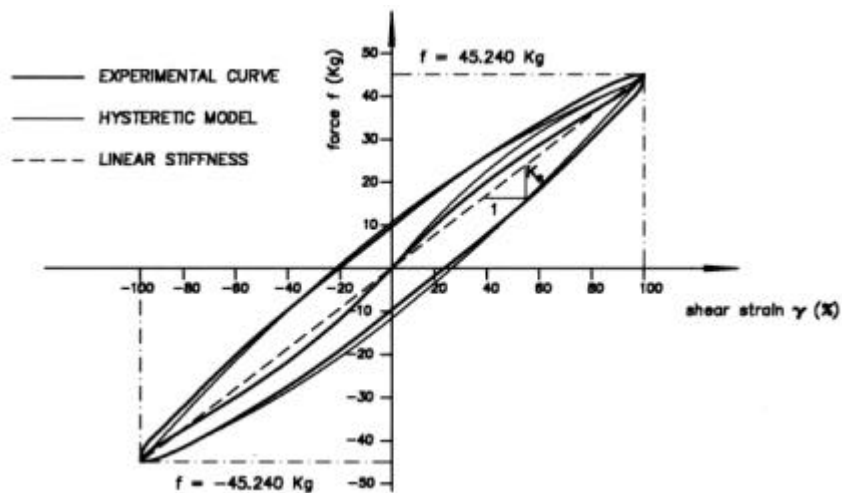


Figure 5. Cycle for maximum shear strain of 100%: comparison between experimental testing and model.

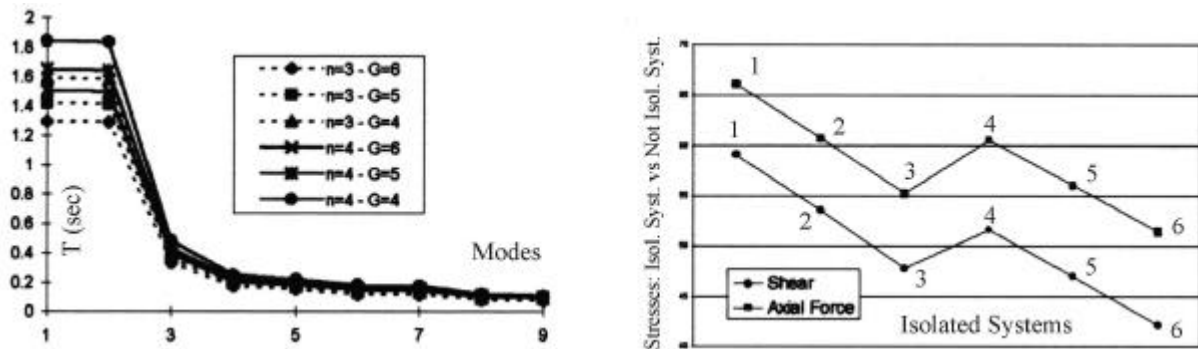


Figure 6. Periods of isolated systems (left); stresses on isolated systems against stresses on non-isolated system (right).

Good results have been obtained for both stresses on the statue, and maximum displacements of the isolators. Spectral acceleration of the first mode of the system is about 45% of the same value of *NIS*; an equal overall reduction of stresses is registered (Fig. 6, right), and no force of traction due to the overturning moment is present on isolating devices. Mean value of relative shear strain ( $\mathbf{g}$ ) of the isolators is 0.933, with a very small dispersion of the values ( $\mathbf{g}_{max}=1.069$ ); with regard to the recorded accelerograms, response of the isolated statue has shown a more significant dispersion of the values:  $\mathbf{g}_{mean}=0.991$ ,  $\mathbf{g}_{max}=1.392$ . In table 1, the most important values that summarize the response of the isolators are shown, in terms of absolute displacement, relative displacements of single isolators, and shear deformation of upper isolators. It should be noted that for those values, stability of the device is verified [9], and auto-centering property of the isolators still applies.

**Table 1. Linear Analysis Results.**

Type of accelerogram	Statistic Values	Max abs. displ. (cm)	Max. rel. displ.	Max. Strain.
Generated Accelerograms	Mean value	9.124	3.006	0.911
	Minimum	8.100	2.687	0.814
	Maximum	10.54	3.487	1.057
	Variance	0.783	0.255	0.077
Recorded Accelerograms	Mean value	9.822	3.270	0.991
	Minimum	6.339	2.121	0.643
	Maximum	13.75	4.579	1.388
	Variance	2.713	0.884	0.268

## NONLINEAR MODEL FOR FORCE-DISPLACEMENT RELATIONSHIP OF ISOLATORS

In the force-displacement relationship of the isolators, the restoring force  $f(x)$  is assumed to be:

$$f(x) = (1 - \mathbf{a}) g(x) + \mathbf{a} z \quad (1)$$

where  $g$  and  $z$  are elastic component and hysteretic component of force  $f$  respectively.  $\mathbf{a}$  is the hysteresis coefficient: for  $\mathbf{a} = 0$  the law is purely elastic, for  $\mathbf{a} = 1$  the law is purely hysteretic. Function  $g(x)$ , which also realizes skeleton curve of the hysteretic relationship, has the following normalized expression [10]:

$$\bar{z} = g(\bar{x}) = \mathbf{r} \bar{x} + \frac{(1 - \mathbf{r}) \bar{x}}{(1 + |\bar{x}|^R)^{1/R}} \quad (2)$$

with  $\bar{z} = z$ ,  $\bar{x} = x$ . Coefficient  $R$  defines curvature near the elastic limit, and  $\mathbf{r}$  the slope of the post-elastic branch of the curve. Hysteretic cycles are described by Masing rules: loading and unloading curves are determined by expression (2) with the assumptions:  $\bar{z} = (z - z_i)/2$ ,  $\bar{x} = (x - x_i)/2$ , where  $(x_i, z_i)$  represents last inversion point. As an example, fig. 7 shows force-displacement diagrams for increasing displacement.

First, influence of  $\mathbf{a}$ ,  $\mathbf{r}$  and  $R$  on  $f(x)$  has been investigated. At this point, it is necessary the introduction of adimensional quantities, ductility  $\tilde{x}$  and adimensional force, defined as:

$$\tilde{f}(\tilde{x}) = f(\tilde{x} x_y) / f_y \quad (3)$$

In the following, tilde will be omitted for clarity. Experimental force-displacement diagram, obtained for rubber isolators, has been used for the calibration of the model parameters,  $\mathbf{a}$ ,  $\mathbf{r}$ , and  $R$ . Passage from adimensional to dimensional quantities is achieved by superimposing the value of secant stiffness at  $f_{100\%}$ , corresponding to  $\mathbf{g}=1$ , value already considered for the determination of equivalent stiffness  $k_e$ . To match the amount of energy dissipation obtained during tests,  $\mathbf{a}$  is set equal to 0.9, and  $R$  to 1.5, since, with this low value, there is dissipation even for small amplitude cycles.

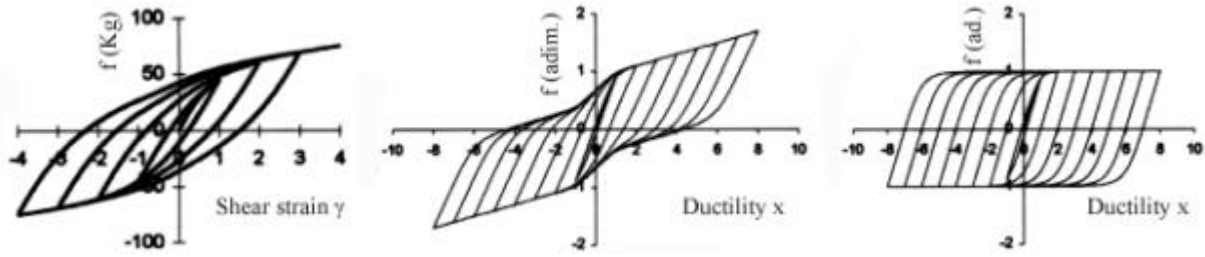


Figure 7. From left to right: adopted hysteretic curve, and curves with different values of parameters: with hardening ( $r=0.1$ ,  $a=0.75$ ), and without hardening ( $r=0$ ,  $a=1$ ).

The values of the parameters determined are:  $x_{100\%}=3.3$  cm,  $f_{100\%}=45.2$  kg,  $a=0.9$ ,  $r=0.05$ ,  $R=1.5$ ; the associated calculated quantities are:  $k_{100\%}=13.709$  kg/cm,  $W_e=74.646$  kg·cm,  $W_d=97.035$  kg·cm,  $\alpha=0.1034$ . With these values a good fitting between experiments and model has been achieved, especially in displacement range 0-100% (Fig. 5) that, in this case, is important because shear strain  $\bar{\epsilon}=1$  is a design value.

### HYSTERETIC RESPONSE OF THE ISOLATED SYSTEM

A parametric analysis has been carried out in order to determine the response sensitivity to characteristics of isolators and seismic force intensity. Motion equation of the hysteretic *SDOF* system, in adimensional form, is:

$$\ddot{x} + 2\mathbf{x} \mathbf{w}_0 \dot{x} + f(x) \mathbf{w}_0^2 = \mathbf{b} \mathbf{w}_0^2 \ddot{x}_g \quad (4)$$

where quantity  $\mathbf{b} = m a_g / f_y$ , defined as the ratio of seismic force intensity to the value of restoring force at yielding.

When hardening exists, for increasing values of  $\mathbf{a}$ , the maximum response in terms of ductility decreases (Fig. 8, top); for  $r=0$ , together with high values of  $\mathbf{b}$  and  $\mathbf{a}$ , response is sensibly higher, because of loss of symmetry. For  $r>0$  resistance increases with displacement and changes qualitatively the response, especially for high values of  $\mathbf{a}$  and  $\mathbf{b}$ : the response is symmetric again and lower than in the other case: see, for example, Fig. 8, center. Parameter  $R$ , that modifies the shape of the  $f(x)$  relationship, especially for  $\mathbf{b}=0.75\div 1.25$ , is important with regard to the maximum value of the response (Fig. 8, bottom), that increases with the decreasing of  $R$ .

In view of the previous results, the response of the isolated statue has been studied as a *SDOF* system (one translational degree of freedom) characterized by an hysteretic restoring force with previously determined parameters. The response has been compared to both linear spatial (*MDOF*) model, and, more directly, to the equivalent linear *SDOF* system. In Fig. 9 condensation of spatial system in the *SDOF* system is shown.

The responses of the above systems show an expected good correlation, as it can be noted in table 2, where results of hysteretic and linear analysis are compared, as well. With artificial accelerograms, the mean value of maximum strains obtained is 1.061, against the linear value  $\bar{g}_{mean}=0.933$  (+14%); those values show an absolute maximum equal to 1.310 (+24% compared to the linear analysis value). With recorded accelerograms, the mean value of maximum strains is 0.945 (-6% compared to the linear analysis value), and absolute maximum is 1.330 (-4%).

Differences between hysteretic analysis results and linear analysis results depend on the shape of the accelerogram, because of the continuous stiffness changes that hysteretic system experiences during motion. Fig. 10 shows the good matching between hysteretic and linear analysis in the initial portion of the response, until, for the first time, the plastic limit is reached. In central portion, where maximum values of response occur, main differences are in the shape of time history; a sensible increase in the period of the hysteretic system can be noted. In the final part, after the excitation is finished, hysteretic response decreases not as quickly as the linear response does, because, for small vibration amplitudes, hysteretic model damping is much lower than the equivalent elastic one. Results show, anyway, that the devices experience a limited entry in plastic field, with absolutely acceptable ductility demand, and a very low level of accelerations transmitted to the statue.

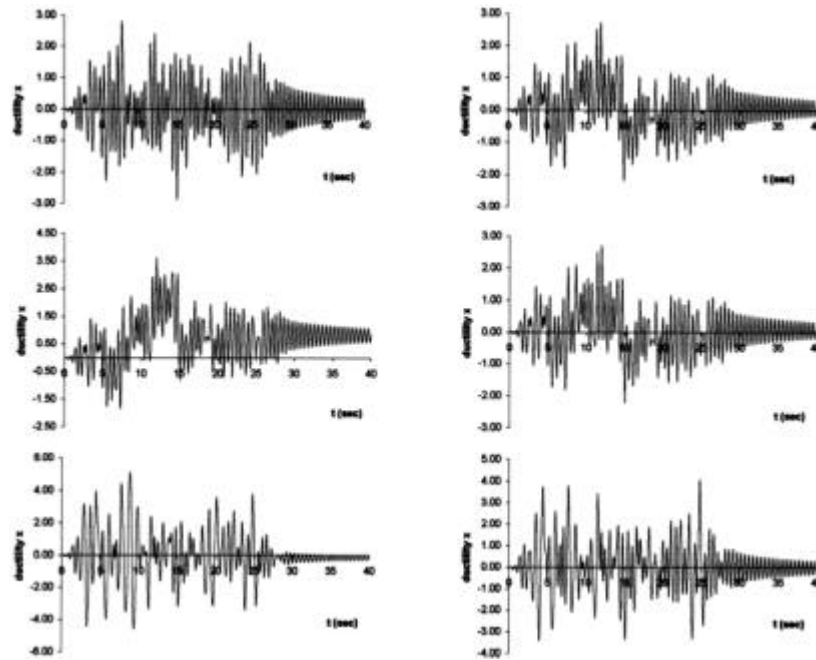


Figure 8. Examples of responses of the hysteretic system.  $r=0.1$ ,  $R=5$ ,  $b=1$ , and  $a=0.5, 1$  (top);  $a=1$ ,  $R=5$ ,  $b=1$ , and  $r=0, 0.1$  (center);  $a=0.5$ ,  $r=0$ ,  $b=1.5$ , and  $R=2, 5$  (bottom).

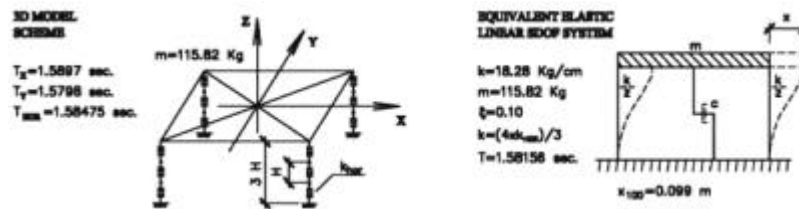


Figure 9. Condensation of linear spatial system in linear *SDOF* system.

Table 2. Comparison between spatial linear system (1), linear *SDOF* system (2), hysteretic system (3).

Accel.	Spat. lin. system (1)		Lin. <i>SDOF</i> syst. (2)		Hysteretic syst. (3)		Comparison between systems			
	$g_{mean}$	$g_{max}$	$g_{mean}$	$g_{max}$	$g_{mean}$	$g_{max}$	$g_{mean2}/g_{mean1}$	$g_{max2}/g_{max1}$	$g_{mean3}/g_{mean2}$	$g_{max3}/g_{max2}$
	(1)		(2)		(3)		(%)	(%)	(%)	(%)
Gener.	0.933	1.069	0.920	1.058	1.061	1.310	98.61	98.97	115.33	123.82
Record.	0.999	1.392	0.988	1.390	0.945	1.330	98.90	99.86	95.65	95.68

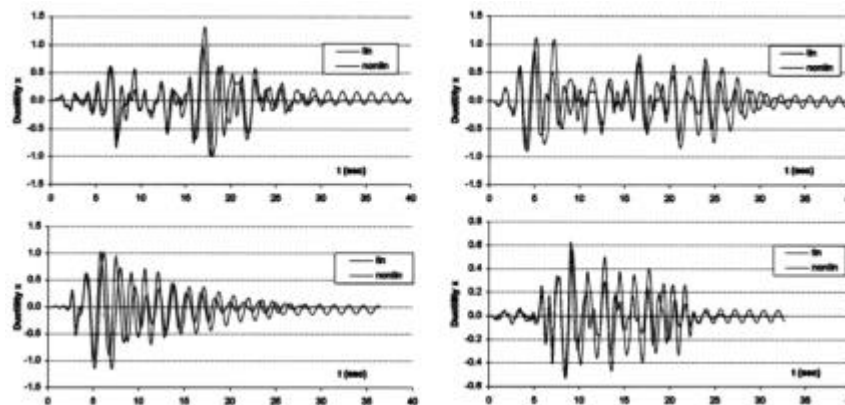


Figure 10. Response in terms of ductility: comparison between hysteretic model and equivalent linear model.

## CONCLUSIONS

Base isolation as the technique to minimize the seismic risk for important statues and similar works has been studied. An hazard evaluation has been performed and the results have been compared with available historic seismic information, international seismic regulations and recent guidelines for isolated structures, in order to determine a reference design spectrum. This spectrum has been compared with the deterministic one (representative of real conditions of the site) obtained following Newmark method. To represent seismic forces in time-domain a set of 12 artificial accelerograms compatible with the assigned spectrum has been generated, and a set of 8 recorded accelerograms has been selected from an ensemble of sixty recent Italian accelerograms.

The isolating device is designed by providing multi-stage high damping laminated rubber bearings. Dynamical characterization of the system has confirmed the good behavior of isolators. The statue shows only rigid translation and rotation, deformation being concentrated only on isolators; participating masses in  $Y$  and  $X$  translations (first two modes) are more than 97%; periods of first two modes are in the range 1.5-1.6 sec against a value of  $T < 0.2$  sec for the system in initial conditions. Spectral acceleration of the first mode of the system is about 45% of the same value of non-isolated system, stability of the device is verified, and auto-centering property of the isolators still applies.

Force-displacement relationship of the isolator has been represented by using an hysteretic model with parameters determined by experimental testing. In view of the good results obtained by using the spatial linear model with equivalent viscous elements, the isolated system has been studied as an hysteretic  $SDOF$  system. Its response, similar to the one of the equivalent linear model, has shown the efficiency of the isolation devices. Required maximum level of displacement under expected seismic forces is absolutely acceptable for isolators, and stresses on the statue are practically negligible.

## ACKNOWLEDGEMENTS

This paper has been partially sponsored by GNDT, C.T.B. 98.03200.PF 54 funds. We are grateful to G. Di Pasquale and A. Pugliese, of the National Seismic Service, for their precious help regarding seismic input.

## REFERENCES

1. Kelly, J.M. 1993. Most Recent Developments on Isolation of Civil Buildings. *Proc. Int. Post-SmiRT Conf. Seminar on Isolation, Energy Dissipation and Control of Vibrations of Structures, Capri, Italy, August, 1993*.
2. Presidenza del Consiglio Superiore dei LL.PP. 1997. Linee guida per la progettazione, l'esecuzione e il collaudo di strutture isolate dal sisma. *Ingegneria Sismica XIV(1)*: pp. 31-48. Bologna: Patron Editore.
3. Pugliese A., Sabetta F. 1987. Attenuation of peak horizontal acceleration and velocity from italian strong-motion records. *Bull. Seism. Soc. Am.* Vol. 77.
4. Eurocode 8: Design provisions for earthquake resistance of structures. UNI ENV 1-1,1-2, 1-3 (1998).
5. Newmark, Hall. 1982. *Earthquake Spectra and Design*. Monograph, Earthquake Engineering Research Institute, Oakland, California, 1982.
6. Vestroni F., Capecchi D., Meghella M., Mazz G., Pizzigalli E. 1992. Dynamic behaviour of isolated buildings. *10th World Conf. Earth. Eng., Madrid, July 1992* Vol. 4: pp. 2473-2478.
7. Morikawa S., Masaki N., Suzuki S., Suizu Y. 1991. Multi-Stage Rubber Bearings for Seismic Isolation. *International Meeting on Earthquake Protection of Buildings, Ancona, giugno 1991*.
8. Kelly J. M., Aiken I. D., Clark P.W. 1997. Experimental testing of reduced-scale seismic isolation bearings for nuclear applications. *EERC, Berkeley 1997*.
9. I. D. Aiken, J. M. Kelly, F. F. Tajirian. 1989. Mechanics of Low Shape Factor Elastomeric Seismic Isolation Bearings. *Report n° UCB/EERC-89/13, nov. 1989*.
10. Vestroni F., Capecchi D. 1997. Coupling and resonance phenomena in dynamical systems with hysteresis. *IUTAM, Symp. on Nonlinear and Chaotic Dynamics in Mechanics, July 27 - August 1, 1997, Cornell University Ithaca, NY*. pp. 203-212. Ed. F.C. Moon, Kluwer Academic Publishers.